Pergamon

Geochimica et Cosmochimica Acta, Vol. 67, No. 16, pp. 3015–3031, 2003

0016-7037/03 $30.00 + .00

doi:10.1016/S0016-7037(03)00273-4

CO_2-H_2O mixtures in the geological sequestration of CO_2. I. Assessment and calculation of mutual solubilities from 12 to 100°C and up to 600 bar

NICOLAS SPYCHER,[1,*] KARSTEN PRUESS,[1] and JONATHAN ENNIS-KING[2]

[1]Lawrence Berkeley National Laboratory, MS 90-1116, 1 Cyclotron Road, Berkeley, CA 94720, USA
[2]CSIRO Petroleum, P.O. Box 3000, Glen Waverley 3150, Australia

(*Received August* 1, 2002; revised 10 April 2003; *accepted in revised form April* 10, 2003)

Abstract—Evaluating the feasibility of CO_2 geologic sequestration requires the use of pressure-temperature-composition (*P-T-X*) data for mixtures of CO_2 and H_2O at moderate pressures and temperatures (typically below 500 bar and below 100°C). For this purpose, published experimental *P-T-X* data in this temperature and pressure range are reviewed. These data cover the two-phase region where a CO_2-rich phase (generally gas) and an H_2O-rich liquid coexist and are reported as the mutual solubilities of H_2O and CO_2 in the two coexisting phases. For the most part, mutual solubilities reported from various sources are in good agreement. In this paper, a noniterative procedure is presented to calculate the composition of the compressed CO_2 and liquid H_2O phases at equilibrium, based on equating chemical potentials and using the Redlich-Kwong equation of state to express departure from ideal behavior. The procedure is an extension of that used by King et al. (1992), covering a broader range of temperatures and experimental data than those authors, and is readily expandable to a nonideal liquid phase. The calculation method and formulation are kept as simple as possible to avoid degrading the performance of numerical models of water-CO_2 flows for which they are intended. The method is implemented in a computer routine, and inverse modeling is used to determine, simultaneously, (1) new Redlich-Kwong parameters for the CO_2-H_2O mixture, and (2) aqueous solubility constants for gaseous and liquid CO_2 as a function of temperature. In doing so, mutual solubilities of H_2O from 15 to 100°C and CO_2 from 12 to 110°C and up to 600 bar are generally reproduced within a few percent of experimental values. Fugacity coefficients of pure CO_2 are reproduced mostly within one percent of published reference data.

1. INTRODUCTION

The potential for global warming caused by the production of carbon dioxide from burning fossil fuels is generating an increasing interest in the study of carbon dioxide sequestration (e.g., U.S. Department of Energy, 1999). One sequestration method currently attracting attention from the scientific community consists of injecting carbon dioxide into saline aquifers (e.g., Pruess and Garcia, 2002), abandoned hydrocarbon reservoirs, or unminable coal seams. Predicting the sequestration potential and long-term behavior of man-made geologic reservoirs requires calculating the pressure, temperature, and composition (*P-T-X*) properties of CO_2-H_2O mixtures at depths where temperatures remain below 100°C, but where pressures may reach several hundred bar. In this *P-T* range, two phases typically coexist: a CO_2-rich gas or liquid phase and an H_2O-rich liquid phase. At temperatures below 100°C, the amount of H_2O in the CO_2-rich phase is quite small, such that the CO_2 properties can be approximated fairly well by those of pure CO_2. In contrast, H_2O in the CO_2-rich phase exhibits a strong nonideal mixing behavior (e.g., Spycher and Reed, 1988; King et al., 1992).

The first task in this study was, therefore, to review existing experimental data on the mutual solubilities of CO_2 and H_2O at temperatures below 100°C and pressures up to 600 bar. The initial focus was more on the H_2O solubility in CO_2 than the solubility of CO_2 in water, because the latter has been the subject of more published investigations. The next step was to implement calculation methods suitable to reproduce the experimental data with sufficient accuracy for the study of geologic CO_2 disposal, but with enough simplicity to avoid degrading the performance of numerical models for which these methods are intended. The present study considers only the two-component system CO_2-H_2O. Because dissolved solids affect the phase partitioning of H_2O and CO_2, further studies are under way to consider the impact of dissolved salts on the mutual solubilities of CO_2 and H_2O.

2. PHASE PROPERTIES IN THE *P-T* RANGE OF GEOLOGICAL CO_2 SEQUESTRATION

The phase diagram of CO_2-H_2O systems has been discussed by numerous authors (Tödheide and Frank, 1963; Takenouchi and Kennedy, 1964; Evelein et al., 1976). However, in this study, only the low-temperature behavior is of interest for applications to geological CO_2 storage. Figure 1 shows the location of all the literature data used in this study on a projection of the CO_2-H_2O phase diagram onto a *P-T* plane. The solid lines are the two- and three-phase coexistence curves explained further below and detailed in Figure 2. Because the intended application of this work is to geological sequestration, the approximate range of pressure and temperature conditions likely to be encountered in such projects is indicated on Figure 1. The lower dotted line indicates typical equilibrium subsurface conditions, based on a mean surface temperature of 20°C, a geothermal gradient of 35°C/km, and a hydrostatic pressure gradient of 105 bar/km. The upper dashed curve indicates typical maximum injection pressures, using a mean surface

* Author to whom correspondence should be addressed (nspycher@lbl.gov).

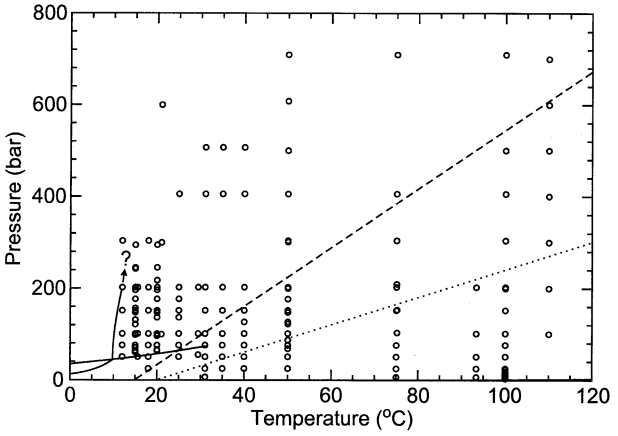

Fig. 1. *P-T* projection of the CO_2-H_2O phase diagram, showing the location of all the literature data points used in this study (open circles). The lower dotted line gives typical equilibrium subsurface conditions (see text). The upper dashed line gives typical maximum injection pressure conditions for geological storage, assuming thermal equilibrium (see text). The solid lines are phase coexistence curves as detailed in Figure 2. The question mark indicates uncertainty about the location of the hydrate formation curve at high pressures.

temperature of 15°C, a geothermal gradient of 25°C/km, and a maximum injection pressure gradient of 160 bar/km. This last curve assumes that the injected CO_2 is at the same temperature as the formation, which should be valid away from the well. Near the well, a lower temperature would be expected. For supercritical conditions, the starting depth of interest is 800 m, which corresponds to a temperature of 35°C using a mean surface temperature of 15°C and a geothermal gradient of 25°C/km.

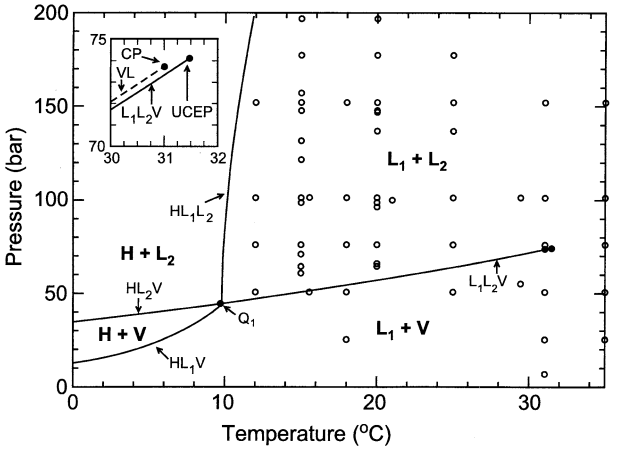

Fig. 2. Enlarged *P-T* projection of the CO_2-H_2O phase diagram, showing the two- and three-phase coexistence curves and the critical points. The circles are literature data points used in this study. The solid curves are three-phase coexistence curves as labeled (vapor phase V, water-rich liquid L_1, CO_2-rich liquid L_2, and hydrate phase H). The dashed line in the inset is the pure-CO_2 liquid-vapor curve (VL), which almost coincides with the three-phase coexistence curve for the CO_2-H_2O system (L_1L_2V). CP is the critical point of pure carbon dioxide, UCEP is the upper critical end point for the CO_2-H_2O system, and Q_1 is a quadruple point for that system.

Most data fall in the subcritical temperature range easily accessible to experimenters (Fig. 1), whereas only ~12% of the data falls in the *P-T* range of most interest for geological storage. Nevertheless, the data outside this range are useful for fitting and validating the representation used here, and they may also be valuable in analyzing possible scenarios in which CO_2 migrates to shallower depths. The question mark in Figure 1 indicates uncertainty about the location of the hydrate formation curve at high pressures, and this uncertainty may cast some doubt on the validity of low temperature solubility measurements in that region.

Figure 2 gives a more detailed view of the two- and three-phase coexistence curves at low temperatures. The various phases involved include a hydrate (H), a water-rich liquid (L_1), a CO_2-rich liquid (L_2) and a vapor phase (V) consisting mostly of CO_2 in the *P-T* range considered. The L_1L_2V and HL_1V curves are based on the representations given by Wendland et al. (1999). The HL_1L_2 curve has been fitted to literature data (Ng and Robinson, 1985; Fan and Guo, 1999), using the functional form $P/P_q = 1 + 32.33\,(T/T_q - 1)^{1/2} + 91.169\,(T/T_q - 1)$ where $T_q = 9.77$°C and $P_q = 44.60$ bar are the *P-T* coordinate of the quadruple point Q_1 at which all four phases coexist. Because the data of Ng and Robinson (1985) for the hydrate formation curve HL_1L_2 only goes up to 140 bar, this representation is not reliable for extrapolation to pressures much above this value. The inset in Figure 2 shows that the vapor-liquid (VL) coexistence curve for pure CO_2 (Span and Wagner, 1996) and the L_1L_2V curve almost coincide. The CO_2 critical point (31.06°C and 73.825 bar from Angus et al., 1976, or 30.978 ± 0.015°C and 73.773 ± 0.003 bar from Span and Wagner, 1996) is very close to the upper critical end point (UCEP, 31.48°C and 74.11 bar, Wendland et al., 1999). Most of the literature data shown in Figure 1 fall either in the L_1L_2 regime, in which a water-rich liquid phase coexists with a CO_2-rich liquid, or in the regime above the critical temperature of CO_2, where the distinction between the vapor and liquid phases of CO_2 disappears.

The narrow three-phase ($L_1 + L_2 + V$) coexistence pressure interval in the CO_2-H_2O system is further illustrated in Figure 3, which shows a *P-X* cross section of the CO_2-H_2O phase diagram at 25°C (i.e., a section perpendicular to the plane of Fig. 2 at 25°C). The inset of this figure was drawn using approximate pressure values. Wendland et al. (1999) report a three-phase coexistence pressure of 64.03 bar at 298.15 K. The pure CO_2 vapor pressure extrapolated at the same temperature (64.32 using data from Angus et al., 1976, or 64.35 from Span and Wagner, 1996) is very close. For the data analysis, the main consequence of this narrow three-phase coexistence pressure interval is that isotherms that cross the L_1L_2V coexistence curve (below 31°C) exhibit a sharp discontinuity in the solubility of H_2O in the CO_2 phase (Fig. 3). Otherwise, the data are continuous. Owing to its narrowness and its location in *P-T* space, the three-phase region is of little importance for geological sequestration, except perhaps for escaping CO_2 which might be at lower pressures and temperatures, and for parts of the CO_2 injection system.

3. REVIEW OF EXPERIMENTAL SOLUBILITY DATA

Most of the early experimental work on CO_2-H_2O mixtures focused on high temperatures and pressures applicable to the

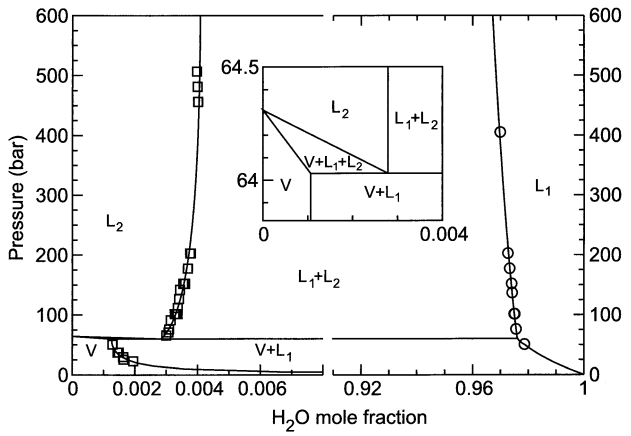

Fig. 3. Pressure-mole fraction cross section of the CO_2-H_2O phase diagram at 25°C. Solid curves are drawn to delimit the various phase coexistence regions: V is the vapor phase, L_1 is the H_2O-rich liquid phase and L_2 is the CO_2-rich liquid phase. Literature data points are shown for CO_2 solubility in H_2O (open circles) and H_2O solubility in CO_2 (open squares) (Wiebe and Gaddy, 1940, 1941; Coan and King, 1971; Gillepsie and Wilson, 1982; King et al., 1992). The inset shows the three-phase coexistence region in greater detail. See text. Note the difference in the horizontal scale between the two parts of the graph.

study of metamorphic processes (typically several hundred degrees Celsius and up to several kilobar) (e.g., Mäder, 1991). Published data in the two-phase region at temperatures below 100°C and at moderate pressures were initially more limited. However, in the last two decades, more data have become available in this *P-T* range. Early studies include those by Wiebe and Gaddy (1939, 1940, 1941), Tödheide and Frank (1963), and Coan and King (1971). More recent work on the two-phase region below 100°C was performed by Gillepsie and Wilson (1982), Briones et al. (1987), Song and Kobayashi (1987), D'Souza et al. (1988), Müller et al. (1988), Sako et al. (1991), King et al. (1992), Dohrn et al. (1993), and Bamberger et al. (2000). Other recent experimental studies providing additional data on the solubility of CO_2 in water (but no information on coexisting gas-phase compositions) within our *P-T* range of interest include those of Teng et al. (1997), Jackson et al. (1995), and Rosenbauer et al. (2001).

Data from all these sources are summarized in Appendix A and tabulated by temperature. Only data points down to 12°C and up to 110°C are listed in Appendix A. Teng et al. (1997) report data at lower temperatures, which we do not consider because of the potential for clathrate formation below 12°C (Fig. 2) (see also Wiebe and Gaddy, 1940; Anderson, 2002). Data at 110°C from the work of Takenouchi and Kennedy (1964) are included in Appendix A and used in discussions later in this paper. Data points above 110°C from these authors and from Müller et al. (1988) are not listed or considered further because they are outside our targeted temperature range.

A number of other experimental studies on CO_2 solubility in water have been conducted besides those listed above. These studies cover pressures mostly below 50 bar and temperatures outside our range of interest, or they do not include data on the composition of the coexisting CO_2-rich phase. For these reasons, data from these studies were not considered. Most of these studies were reviewed by Crovetto (1991) and Carroll and Mather (1992) to derive Henry's law constants for CO_2 in water. As discussed later, solubilities calculated in the present study, using data in Appendix A, generally agree well with those calculated by these authors.

The mutual solubilities of H_2O and CO_2 from 12 to 110°C and up to 600 bar (in Appendix A) are shown as symbols on Figures 4 to 7. Data on these figures correspond to the branches of the *P-X* phase diagram shown with superposed symbols on Figure 3. Curves show solubilities calculated using methods discussed later. Measured aqueous CO_2 solubilities define clear trends (right side of Figs. 4–7), with the points of overlapping data sets generally agreeing within a few percent or falling in trend with each other. The same is true for H_2O solubilities in the CO_2-rich phase, but only at low temperatures (left side of Figs. 4–6). H_2O solubilities reported at 50, 75, and 100°C show more relative spread (left side of Figs. 6–7). Some assessment of precision between different data sets can be made from the number of significant digits reported for solubility values in Appendix A. However, the most precise measurements may not necessarily be the most accurate if systematic measurement errors affected these data. A full evaluation of experimental errors and uncertainties affecting these data was beyond the scope of this study. However, because the relative spread of the majority of these data remains within our targeted range of data reproducibility (a few percent), a better knowledge of data uncertainty would unlikely affect the outcome of this study. Some observations regarding these solubility data follow.

The H_2O solubilities reported by Tödheide and Frank (1963) at 50 and 100°C plot quite off-trend (Fig. 6), but were reported with a large error margin (±1 mol.%). Other solubilities least in line with the bulk of the data (Figs. 4–7) include H_2O solubilities reported by D'Souza et al. (1988) at 50°C, and by Gillepsie and Wilson (1982) and Sako et al. (1991) at 75°C (Fig. 6). CO_2 solubilities measured by Gillepsie and Wilson (1982) at 15°C (Fig. 4) and by Sako et al. (1991) at 75°C (Fig. 6) also fall somewhat off-trend. H_2O solubilities from Greenwood and Barnes (1966) at 100°C (Fig. 6) appear to have been extrapolated and were not included in Appendix A (these authors cite Wiebe and Gaddy, 1939, 1940, 1941, as sources of the 100°C data; however, Wiebe and Gaddy did not report gas-phase compositions above 75°C).

As discussed previously, the sharp discontinuity in H_2O solubility at subcritical temperatures (Figs. 4 and 5) coincides with the phase change from a gaseous to a liquid CO_2-rich phase. The pressure interval over which three phases coexist (H_2O-rich liquid, CO_2-rich gas, and CO_2-rich liquid) is very small (Figs. 2 and 3) and, using only the solubility data, is difficult to distinguish from the saturation pressure of pure CO_2 at any given temperature (see Wendland et al., 1999, for measurements on the three-phase coexistence line). Above this saturation pressure (or more precisely above this three-phase pressure interval), the H_2O solubility in the CO_2-rich phase increases with pressure and temperature (Figs. 5–7). As would be expected, above the critical temperature the H_2O solubility trend with pressure becomes progressively smoother.

The solubility of CO_2 decreases with rising temperature, but increases sharply with rising pressure up to the saturation pressure and at a lesser rate thereafter (Figs. 4–7). Below the critical temperature, the CO_2 solubility trend with pressure

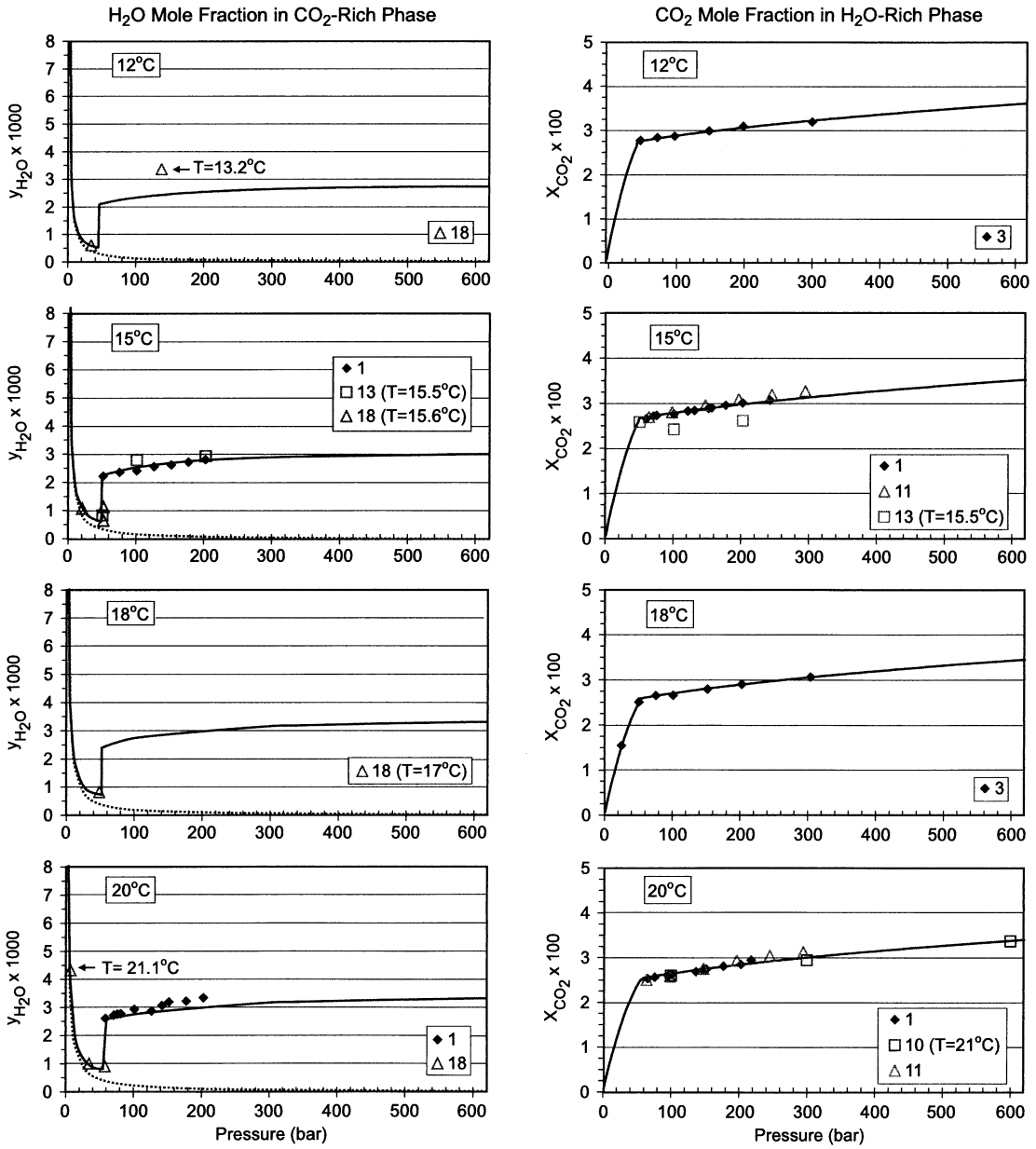

Fig. 4. Mutual solubilities of H_2O and CO_2 at 12, 15, 18, and 20°C and pressures to 600 bar. Experimental data (Appendix A) are shown as symbols, with sources given below. Solubilities computed using Eqn. 11 to 14, B1 and B7 and parameters in Tables 1 and 2 are shown as solid lines. The dotted lines are calculated assuming ideal mixing. See text and Appendix B. Reference numbers for this figure and Figures 5 to 7 are as follows: (1) King et al. (1992), (2) Wiebe and Gaddy (1941), (3) Wiebe and Gaddy (1940), (4) Wiebe and Gaddy (1939), (5) Coan and King (1971), (6) Tödheide and Frank (1963), (7) Takenouchi and Kennedy (1964), (8) Jackson et al. (1995), (9) Greenwood and Barnes (1966), (10) Rosenbauer et al. (2001), (11) Teng et al. (1997), (12) Müller et al. (1988), (13) Gillepsie and Wilson (1982), (14) Briones et al. (1987), (15) D'Souza et al. (1988), (16) Sako et al. (1991), (17) Dohrn et al. (1993), (18) Song and Kobayashi (1987), (19) Bamberger et al. (2000).

reflects two solubility curves for two distinct phases: liquid CO_2 above saturation pressures, and gaseous CO_2 below these pressures. This results in a sharp break in slope on each of the overall solubility trends at subcritical temperatures. Above the critical temperature, the CO_2 solubility trend reflects only one solubility curve for gaseous CO_2, with a bend in the vicinity of the critical point that smoothly diminishes away from this point (Fig. 5). At the critical point, the solubilities of liquid and gaseous CO_2 in water should be equal.

4. SOLUBILITY MODEL

Correlations to compute the mutual solubilities of CO_2 and H_2O have been developed by many authors. Solubility models

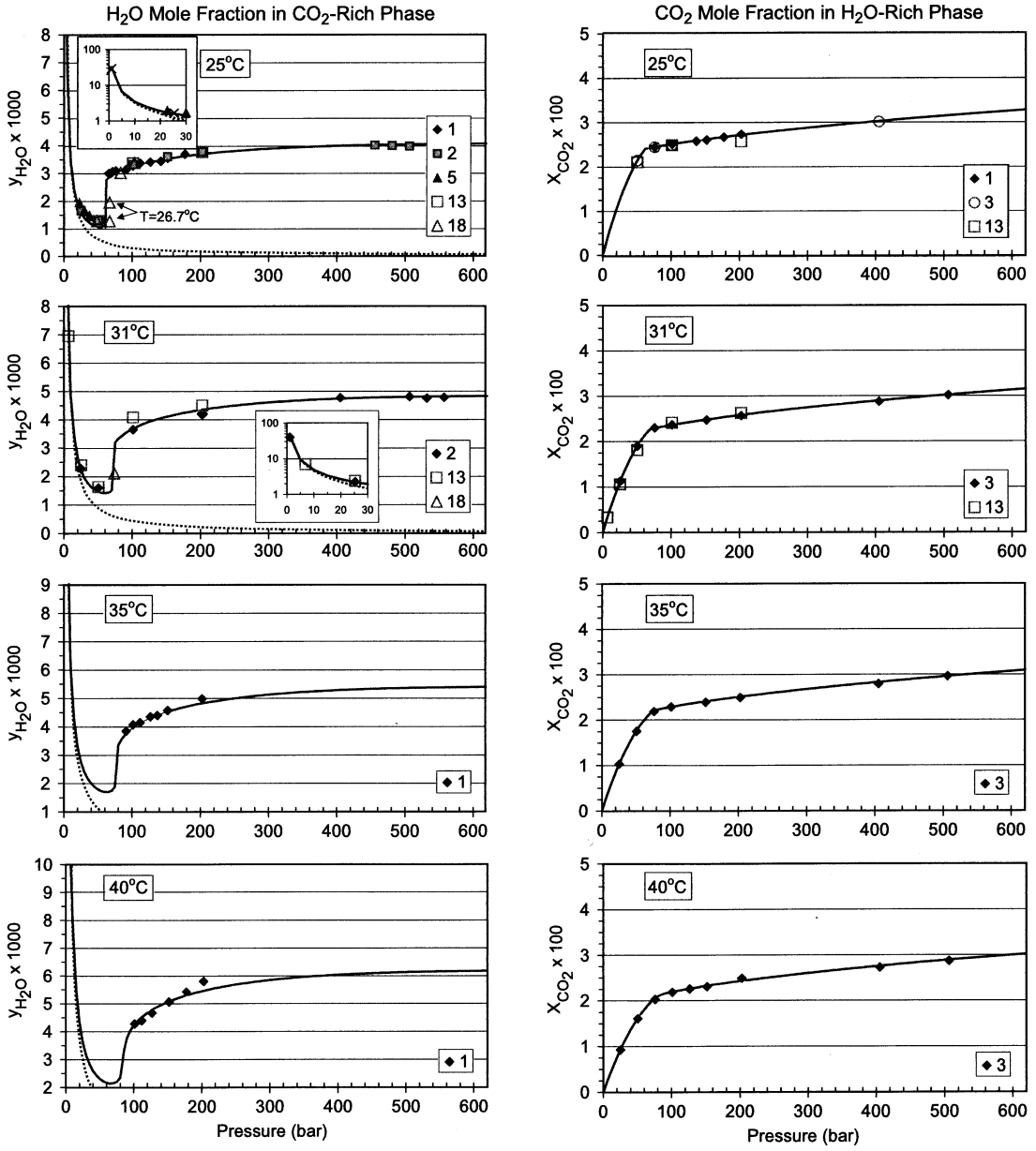

Fig. 5. Mutual solubilities of H_2O and CO_2 at 25, 31, 35, and 40°C and pressures to 600 bar. Solid lines are calculated data. See caption of Figure 4 for complete legend and data sources.

published in the last decade include those by King et al. (1992), Duan et al. (1992), as implemented in their website calculator (http://geotherm.ucsd.edu/geofluids/), Shyu et al. (1997), and Bamberger et al. (2000). Various other authors have developed methods to express *P-T-X* properties of two-phase CO_2-H_2O mixtures (e.g., Coan and King, 1971; Spycher and Reed, 1988) and to calculate the solubility of CO_2 in water (e.g., Müller et al., 1988; Crovetto, 1991; Carroll and Mather, 1992). All these studies, however, either do not cover our entire *P-T* range of interest or involve correlations that are more complex or less accurate (with respect to solubility) than those presented below. Furthermore, existing solubility models that do overlap the *P-T* range considered here do not rely on a large number of experimental data points for both the CO_2-rich and H_2O-rich phases.

4.1. Thermodynamic Formulation

The standard approach for calculating the mutual solubilities of liquids and compressed gases (by equating the fugacities of phases at equilibrium) is thoroughly described in the chemical engineering literature (e.g., Prausnitz et al., 1986). Here, we use a similar approach derived from equating chemical potentials, but using conventions and standard states more typical of aqueous geochemistry studies (e.g.,

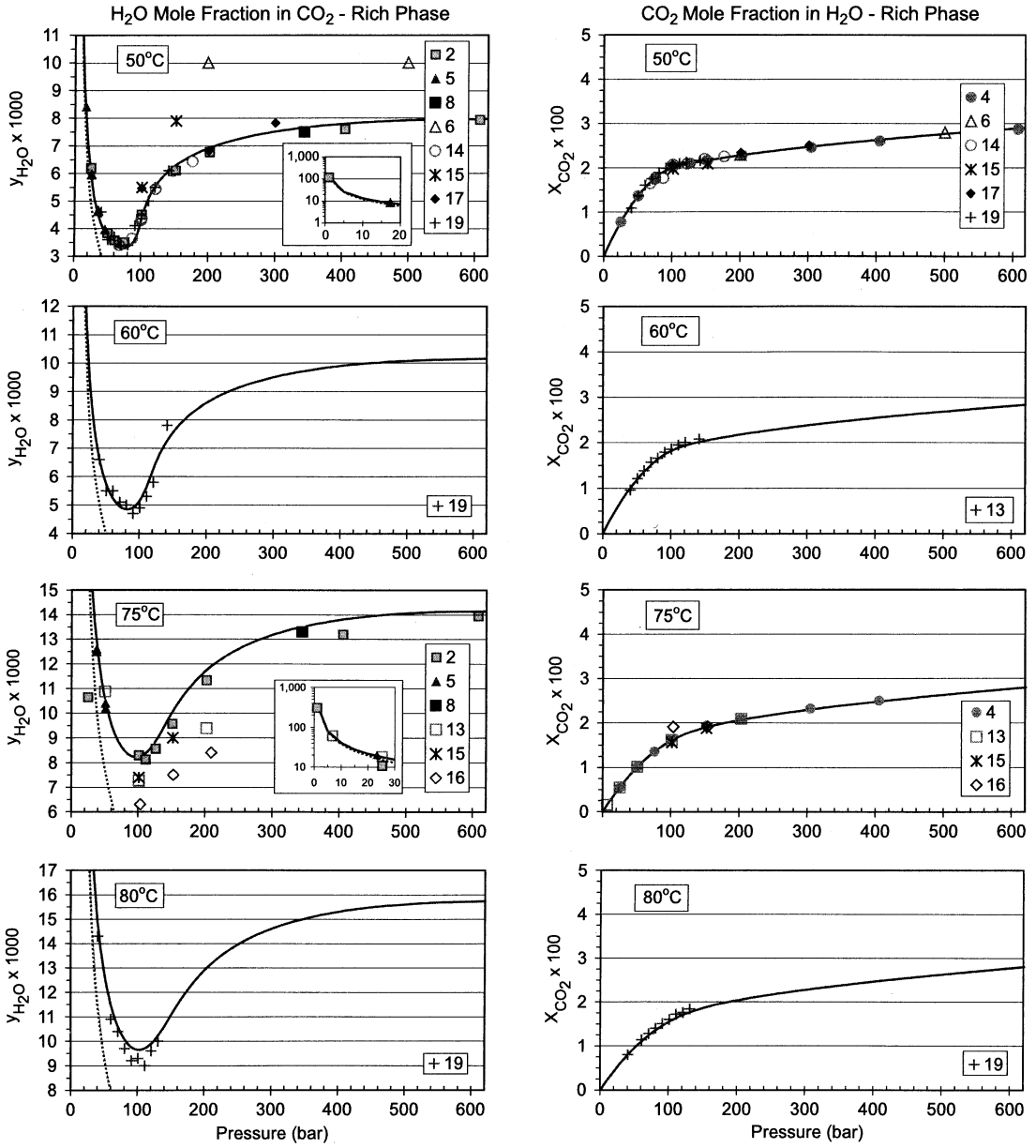

Fig. 6. Mutual solubilities of H_2O and CO_2 at 50, 60, 75, and 80°C and pressures to 600 bar. Solid lines are calculated data. See caption of Figure 4 for complete legend and data sources.

Helgeson and Kirkham, 1974; Helgeson et al., 1981; Johnson et al., 1992). These call for unit activity of pure liquids at all pressures and temperatures; for gases, unit fugacity of the hypothetical gas at 1 bar and any temperature; and for aqueous CO_2, unit activity in a hypothetical one molal solution referenced to infinite dilution at any pressure and temperature. In addition, our approach relies on "true" equilibrium constants (K) (i.e., directly related to the standard Gibbs free energy of reaction as $\Delta G^0 = -RT \ln K$; e.g., Denbigh, 1983) rather than the Henry's law constants (K_H) typically used in the chemical engineering literature. Because equilibrium constants, as used here, are more fundamental thermodynamic properties than Henry's law constants, the formulation can be more easily extended to a non-ideal aqueous phase (i.e., resulting from the addition of salts) than formulations involving Henry's law constants.

At equilibrium, the following reactions and corresponding equilibrium constants can be written:

$$H_2O_{(l)} \Leftrightarrow H_2O_{(g)} \quad K_{H2O} = f_{H2O(g)}/a_{H2O(l)} \tag{1}$$

$$CO_{2(aq)} \Leftrightarrow CO_{2(g)} \quad K_{CO2(g)} = f_{CO2(g)}/a_{CO2(aq)} \tag{2}$$

where K are "true" equilibrium constants as defined above, f are fugacities of the gas components, and a are activities of com-

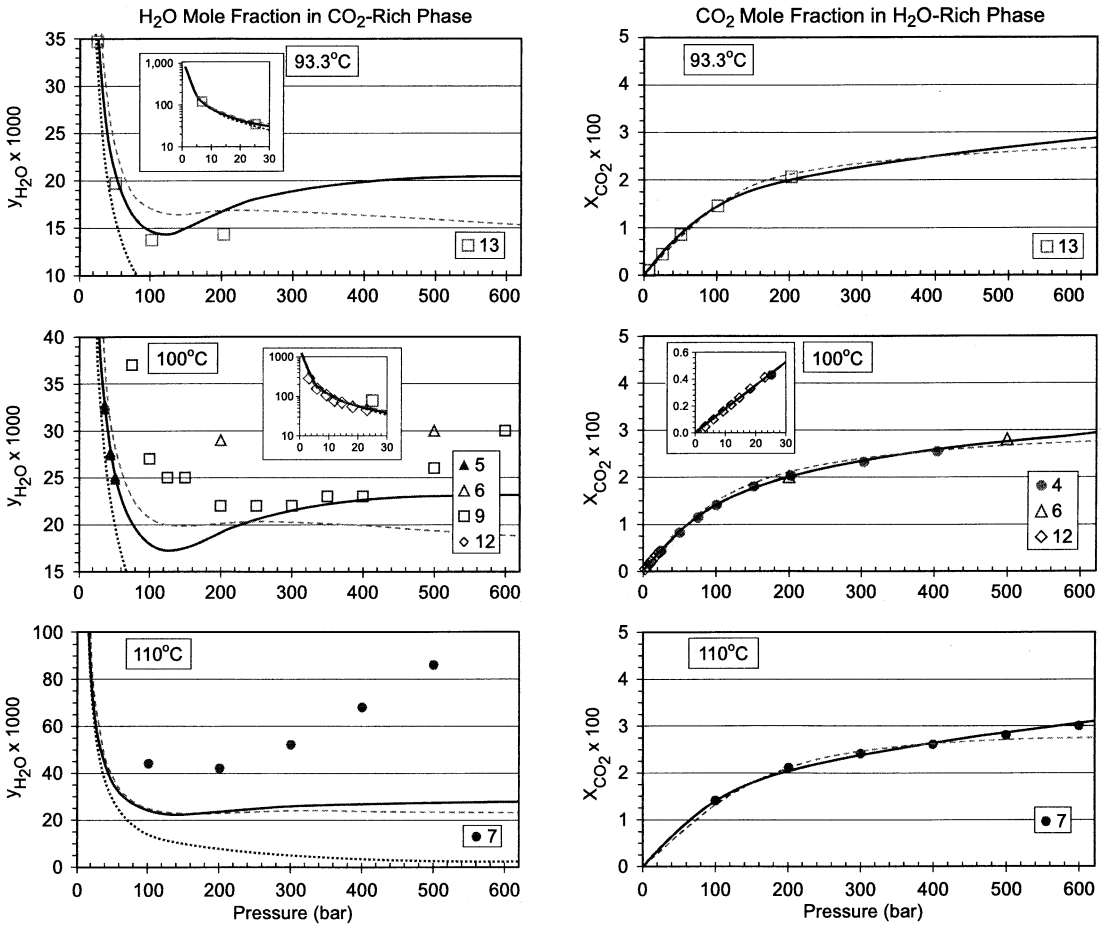

Fig. 7. Mutual solubilities of H_2O and CO_2 at 93.3, 100, and 110°C and pressures to 600 bar. Solid lines are calculated data. Dashed lines are results from Geofluids (Duan et al., 1992, as implemented in their website calculator http://geotherm.ucsd.edu/geofluids/). See caption of Figure 4 for complete legend and data sources.

ponents in the liquid (aqueous) phase.[1] Values of K_{H2O} and $K_{CO2(g)}$ vary with temperature and pressure. The temperature dependence is taken into account by expressing these equilibrium constants as a polynomial function of temperature (at one bar, and H_2O saturation pressures above 100°C). The pressure correction (at a given temperature) is approximated by

$$K_{(T,P)} = K^0_{(T,P^o)} \exp\left(\frac{(P-P^0)\,\bar{V}_i}{RT}\right) \quad (3)$$

where $\bar{V}_i$ is the average partial molar volume of the pure condensed component i over the pressure interval P^0 to P, and P^0 is a reference pressure, here taken as 1 bar (and H_2O saturation pressure above 100°C). Because $\bar{V}_i$ also varies with temperature (much less than with pressure), $\bar{V}_i$ is also averaged over the temperature range of interest so that $K_{(T,P)}$ values can be approximated from one constant $\bar{V}_i$ value for each component. Eqn. 3 derives directly from the fundamental relationship expressing the change in chemical potential with pressure $(\partial\mu/\partial P)_T = V$, and its exponential term is similar in form to the "Poynting" factor described in the chemical engineering literature (e.g., Prausnitz et al., 1986). Eqn. 3 yields a correction typically $< 10\%$ below 100 bar, but this correction becomes significantly larger at higher pressures. As discussed later, values of K^0_{H2O}, K^0_{CO2}, $\bar{V}_{H2O}$ and $\bar{V}_{CO2}$ can be taken directly from the literature and/or fitted to experimental solubility data.

If CO_2 changes from a gaseous to a liquid state as pressure increases (at subcritical temperatures), additional free-energy terms related to the phase transition need to be added to Eqn. 3. However, one alternative to adding extra terms in Eqn. 3 is to consider another equilibrium constant in this equation, $K^0_{CO2(l)}$, referring to liquid instead of gaseous CO_2. This equilibrium constant is then used in place of $K^0_{CO2(g)}$ when the temperature is subcritical and the pressure is above the CO_2 saturation pressure, with the values of $K^0_{CO2(l)}$ and $K^0_{CO2(g)}$ being equal at the critical temperature. This is the approach adopted in this study. Also, the dissociation of $CO_{2(aq)}$ to bicarbonate (HCO_3^-) can be safely ignored because the pK for this reaction at the temperatures considered here ranges between ~6.0 and 6.6, whereas the solution pH at the CO_2 pressures considered is < 4.

[1] In these equations, by convention, the fugacity f represents f/f^0 with $f^0 = 1$ bar, and the activity a is on a mole fraction scale for water and a molality scale for aqueous CO_2.

From the definition of fugacity and partial pressures (e.g., Hala et al., 1967, Denbigh, 1983; Prausnitz et al., 1986), we can write

$$f_i = \phi_i y_i P_{tot} \tag{4}$$

where f_i, Φ_i and y_i are the fugacity, fugacity coefficient, and mole fraction of component i in the gas phase, respectively, and P_{tot} is the total pressure (the partial pressure $P_i = y_i P_{tot}$). (Note: hereafter, y always denotes mole fractions in the CO_2-rich phase, whereas x is used for mole fractions in the aqueous phase). Substituting Eqn. 4 in Eqn. 1 and 2 then yields

$$f_{H2O} = \phi_{H2O} y_{H2O} P_{tot} = K_{H2O} a_{H2O(1)} \tag{5}$$

$$f_{CO2} = \phi_{CO2} y_{CO2} P_{tot} = K_{CO2(g)} a_{CO2(aq)} \tag{6}$$

Recasting Eqn. 5 to express the water mole fraction in the gas phase and applying the pressure correction to K_{H2O} from Eqn. 3 yields

$$y_{H2O} = \frac{K^0_{H2O} a_{H2O}}{\phi_{H2O} P_{tot}} \exp\left(\frac{(P-P^0)\bar{V}_{H2O}}{RT}\right) \tag{7}$$

A fairly good approximation (within 10% in our considered P-T range) of water mole fractions in the CO_2-rich phase can be computed with this equation if a_{H2O} is assumed to be unity. However, for better accuracy at high pressures, the water activity deviation from unity caused by dissolved CO_2 should be taken into account. At the pressures and temperatures considered here, the CO_2 solubility is sufficiently small such that Raoult's law can be used to set the water activity (a_{H2O}) equal to its mole fraction in the water phase (x_{H2O}). For a system where H_2O and CO_2 are the only two components, x_{H2O} is directly calculated as $1 - x_{CO2}$, such that

$$y_{H2O} = \frac{K^0_{H2O}(1-x_{CO2})}{\phi_{H2O} P_{tot}} \exp\left(\frac{(P-P^0)\bar{V}_{H2O}}{RT}\right) \tag{8}$$

The mole fraction of aqueous CO_2 (x_{CO2}) is computed from its molality m (i.e., mol/kg$_{H2O}$, such that $x_{CO2} = m_{CO2}/[m_{CO2} + 55.508]$ with the convention that $a_{CO2} = \gamma m_{CO2}$, where γ is the activity coefficient of dissolved CO_2 on a molality scale). For this electrically neutral species, if no salts are present, the activity coefficient is set to $\gamma = 1/(1 + m_{CO2}/55.508)$, which is a molality to mole fraction correction (e.g., Helgeson et al., 1981; Denbigh, 1983) yielding a unit activity coefficient on the mole fraction scale. Further correction for nonideality is not considered at this stage because the solubility of CO_2 in water is small. These relationships yield

$$a_{CO2} = 55.508\, x_{CO2} \tag{9}$$

Substituting Eqn. 3 and 9 into Eqn. 6 gives

$$x_{CO2} = \frac{\phi_{CO2}(1-y_{H2O})\, P_{tot}}{55.508 K^0_{CO2(g)}} \exp\left(-\frac{(P-P^0)\bar{V}_{CO2}}{RT}\right) \tag{10}$$

Eqn. 8 and 10 have essentially the same form as those typically derived in the chemical engineering literature (e.g., Prausnitz et al., 1986; King et al., 1992), except that the fugacities are expressed through the use of true equilibrium constants and the activities of liquid H_2O and aqueous CO_2 (using the conventions described earlier). These equations can be solved directly by setting

$$A = \frac{K^0_{H2O}}{\phi_{H2O} P_{tot}} \exp\left(\frac{(P-P^0)\bar{V}_{H2O}}{RT}\right) \tag{11}$$

and

$$B = \frac{\phi_{CO2} P_{tot}}{55.508\, K^0_{CO2(g)}} \exp\left(-\frac{(P-P^0)\bar{V}_{CO2}}{RT}\right) \tag{12}$$

such that

$$y_{H2O} = \frac{(1-B)}{(1/A-B)} \tag{13}$$

Eqn. 13 provides the water solubility in the CO_2-rich phase. This equation simplifies to $y_{H2O} = A$ if the term B is neglected (which corresponds to the assumption of unit water activity, as discussed earlier for Eqn. 7). Knowing y_{H2O}, the aqueous CO_2 mole fraction is then given by

$$x_{CO2} = B(1-y_{H2O}) \tag{14}$$

Because y_{H2O} is typically small (Figs. 4–7), fairly good approximations of x_{CO2} (within an error equal to y_{H2O}) can be computed by setting $x_{CO2} = B$. In our case, however, the full forms of Eqn. 13 and 14 are used. Because a direct method is used to compute fugacity coefficients (below), these two equations are solved without iterations.

As mentioned earlier, at subcritical temperatures and pressures above saturation values, $K^0_{CO2(g)}$ in Eqn. 12 needs to be replaced with another equilibrium constant, $K^0_{CO2(l)}$, referring to liquid instead of gaseous CO_2. The method implemented here uses $K^0_{CO2(l)}$ in place of $K^0_{CO2(g)}$ when both the following conditions are met: (1) temperature is below 31°C (rounded-off value of the critical temperature of pure CO_2) and (2) the calculated volume of the compressed gas phase (Appendix B) is < 94 cm^3/mol (rounded-off value of the critical volume of pure CO_2). In doing so, the calculated phase-change boundary for the CO_2-rich phase is assumed the same as for pure CO_2, and the P-T space in which three phases coexist (CO_2 gas, CO_2 liquid, and H_2O liquid) is ignored. This approximation can be justified because the three-phase P-T space is quite small and, in fact, essentially indiscernable using the available experimental solubility data (Figs. 2 and 3).

4.2. Equation of State

The fugacity coefficients in Eqn. 11 and 12 must be derived from the P-V-T or P-T-X properties of H_2O and CO_2 mixtures, preferably using an equation of state. Equations of state and mixing rules with various degrees of complexity and accuracy have been presented in the literature to calculate properties of CO_2-H_2O mixtures. Duan et al. (1992) developed an equation of state including a fifth-order virial expansion in volume. Their equation is applicable from 50 to 1000°C and up to 1000 bar and is quite accurate. However, its complex form was deemed undesirable for our purpose, which was to implement the simplest correlations possible, preferably not requiring an iterative solution. Spycher and Reed (1988) presented a virial equation strictly in terms of pressure and temperature, which has the

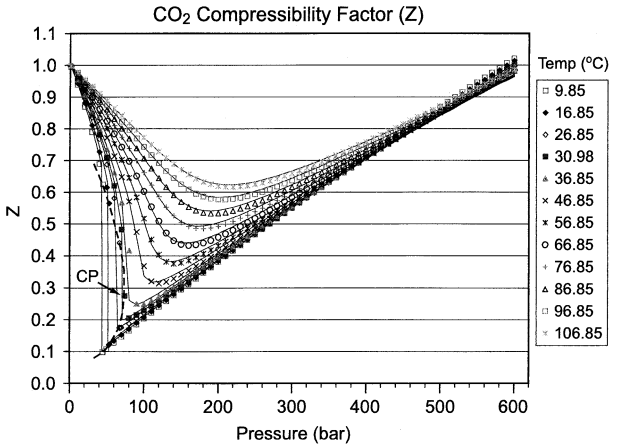

Fig. 8. Compressibility factor of pure CO_2 between 9.85 and 106.85°C (283–380 K) up to 600 bar. Reference data (symbols) are from Lemmon et al. (2003). Values computed using Eqn. B1 and parameters in Table 1 are shown as solid lines. See text and Appendix B.

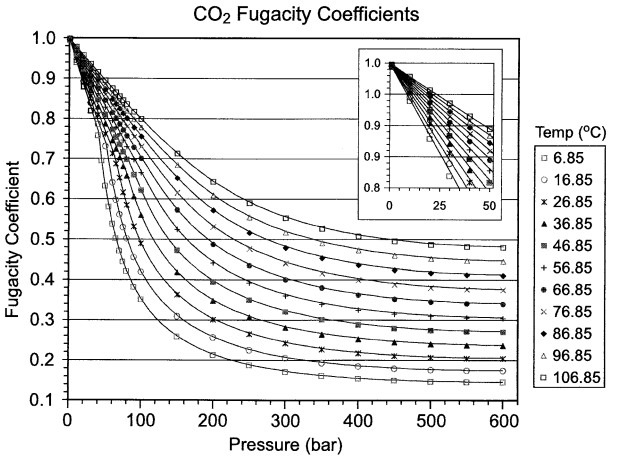

Fig. 9. Fugacity coefficient of pure CO_2 between 6.85 and 106.85°C (280–380 K) up to 600 bar. Reference data (symbols) are from Angus et al. (1976). Values computed using Eqn. B1 and B7 and parameters in Table 1 are shown as solid lines. See text and Appendix B.

advantage of being efficiently implemented in numerical models where pressure and temperature are primary variables. However, their equation uses only two virial coefficients and is of limited use below 100°C and unsuitable for the two-phase region or in the vicinity of the critical point. Preference was given to cubic equations in volume (i.e., of the Van-der-Waals type) such as those developed by Redlich and Kwong (1949) and Peng and Robinson (1976). These equations are simple and generally accurate enough for practical applications.

The Redlich-Kwong equation and its various modifications have been used successfully to represent the properties of CO_2-H_2O mixtures over various *P-T* ranges (e.g., deSantis et al., 1974; Kerrick and Jacobs, 1981; King et al., 1992). Such equations, together with standard mixing rules, have a limited accuracy in the vicinity of the critical point. However, they have the advantage of representing properties of gases and their mixtures fairly well over significant *P-T* ranges using relatively simple expressions. For example, using a Redlich-Kwong equation fitted to their data, King et al. (1992) were able to represent within a few percent their experimental solubility data and those of Wiebe and Gaddy (1940, 1941) from 15 to 40°C and up to 500 bar. The Peng-Robinson equation is somewhat more elaborate than the Redlich-Kwong equation, but has the advantage of reproducing the liquid-vapor boundary much more accurately than the Redlich-Kwong equation. Shyu et al. (1997) used the Peng-Robinson equation and sophisticated mixing rules to represent CO_2-H_2O mutual solubilities from 25 to 350°C and up to 1000 bar. These authors' predictions showed generally good agreement with limited published experimental data, although from their paper it was difficult to evaluate the accuracy of their model below 100°C. Bamberger et al. (2000) also used a Peng-Robinson equation with simple mixing rules to fit their experimental solubility data at 50, 60, and 80°C and up to 141 bars.

In this study, good results (Figs. 4–9) were obtained using a modified Redlich-Kwong equation, with the intermolecular attraction parameter assumed to vary linearly with temperature (Appendix B). Standard mixing rules were applied but simplified by assuming infinite H_2O dilution in the CO_2-rich phase (i.e., setting $y_{H2O} = 0$ in the mixing rules) (Appendix B). In doing so, simple correlations were obtained, and an iterative procedure to solve Eqn. 13 and 14 was not required (Appendix B). By assuming infinite H_2O dilution, the volume of the gas phase and the fugacity coefficient of CO_2 in the gas mixture are approximated as those of pure CO_2. The presence of H_2O in the compressed gas phase is assumed to have no effect on the much more abundant CO_2 molecules, although the strong effect of CO_2 on H_2O molecules is taken into account (Appendix B). King et al. (1992) successfully applied this approach at low temperatures (15–40°C). In this study, we applied this approach with good results over our entire *P-T* range of interest. The only Redlich-Kwong parameters needed to implement this method are the attraction and repulsion parameters for pure CO_2 (a_{CO2} and b_{CO2}), the repulsion parameter for pure water (b_{H2O}), and the H_2O-CO_2 binary interaction parameter ($a_{H2O\text{-}CO2}$) (Appendix B). These parameters were fitted to available reference *P-V-T* data for pure CO_2 (Span and Wagner, 1996) and to the *P-T-X* data in Appendix A, as discussed later.

Cubic equations of state typically cannot represent *PVT* behavior with great accuracy. As already pointed out by others (e.g., Shyu et al., 1997), tuning these equations to experimental or reference data, as done here, can provide good predictions of *P-T-X* phase equilibria, but saturation volumes often deviating significantly from measured data. In this study, the compressibility factor ($Z = \frac{PV}{RT}$) for pure CO_2 was represented with enough accuracy (typically $< 5\%$) (Fig. 8) to reproduce fugacity coefficients mostly within one percent of published reference data (Fig. 9), as discussed later. However, the *P-T* saturation curve could only be reproduced within a few bars from reference data.

To improve predictions of the *P-T* saturation curve, the approach outlined above was also implemented using the Peng-Robinson equation (in its standard form, with molecular interaction parameters derived from critical constraints). This equation is known to yield more accurate vapor pressures than the

Table 1. Fitted Redlich-Kwong parameters for Eqn. B1 to B7 (Appendix B). Values of b_{H2O} and $a_{H2O\text{-}CO2}$ were derived assuming infinite dilution of H_2O in the compressed gas phase (i.e. $y_{H2O} = 0$ and $y_{CO2} = 1$ in the mixing rules; a value for a_{H2O} is not needed). See text. The uncertainty shown represents the 95% confidence interval from the model calibration.

Parameter	Value	Units
a_{CO2}	7.54×10^7–$4.13 \times 10^4 \times T$(K) (fitted T range: 283–380K)	bar cm^6 K$^{0.5}$ mol^{-2}
	T (°C) / a_{CO2} ($\pm 0.01 \times 10^7$)	
	15 / 6.35×10^7	
	25 / 6.31×10^7	
	50 / 6.21×10^7	
	75 / 6.10×10^7	
	100 / 6.00×10^7	
b_{CO2}	27.80 (± 0.01)	cm^3/mol
b_{H2O}	18.18 (± 1.05)	cm^3/mol
$a_{H2O\text{-}CO2}$	7.89×10^7 ($\pm 0.08 \times 10^7$)	bar cm^6 K$^{0.5}$ mol^{-2}

Redlich-Kwong equation. In doing so, the CO_2 vapor pressure was indeed better reproduced (within 0.3 bar of reference data). However, absolute deviations above the critical point were on the average twice as large as with the Redlich Kwong equation. Below the critical point, a few bars away from the saturation curve, deviations were on the average roughly the same. Modifications of the Peng-Robinson equation from Melhem et al. (1989) did not produce significantly better results in our *P-T* range of interest. For this reason, preference was given to our original approach, keeping in mind that the goal of this study was to represent accurately (within a few percent), yet simply, available solubility data at elevated pressures, and not to predict accurate volumetric properties in the vicinity of the CO_2 saturation curve.

4.3. Model Calibration

The solubility model was implemented as a computer routine (Spycher and Pruess, in preparation).[2] Parameters needed for implementation of this model (Tables 1 and 2) were obtained from the literature, where available, and by calibration (fitting procedure) to the data in Appendix A, as well as to other published reference data as discussed below. Model calibration was performed automatically using the PEST-ASP v5.0 freeware, a powerful model-independent nonlinear parameter estimation package (Doherty, 2002). Mutual solubility points above ~600 bar and 100°C (beyond our range of interest), those within a few bars from the CO_2 saturation pressure curve, and those clearly off the general trend were given lower weights than other points to avoid biasing the calibration by large deviations. In doing so, solubilities could be reproduced generally within a few percent of experimental values over a temperature range from 12 to 110°C for x_{CO2} and from 15 to 100°C for y_{H2O}, to pressures of 600 bar.

Values of K^0_{H2O} were regressed as a polynomial function of temperature using the fugacity values of pure H_2O at 1 bar from Harvey et al. (2000) (Table 2). These are reference data from the National Institute of Standards and Technology (NIST) computed as reported in Wagner and Pruβ (2002). The average partial molar volume of water ($\bar{V}_{H2O}$) was also calculated using these reference data (average of values over a *P-T* grid of 1–601 bar by 280–380 K using 10-bar and 10-K increments) (Table 2). These data yielded satisfactory results that could not be significantly improved by further adjustments through calibration.

King et al. (1992) derived Redlich-Kwong molecular interaction parameters and other data necessary to compute CO_2-H_2O mutual solubilities (from experimental data at 15–40°C and up to 200 bar), but their parameters were not suitable for our broader temperature and pressure range. The Redlich-Kwong parameters for pure CO_2 (a_{CO2} and b_{CO2}) were obtained by fitting Eqn. B1 and B2 (Appendix B) to compressibility factors from Lemmon et al. (2003) from 283 to 380 K (9.85 to 106.85°C) and from 1 to 600 bar (NIST data calculated from Span and Wagner, 1996). Ignoring errors for points within a couple bars from the vapor pressure curve, these compressibility factors were reproduced with a mean absolute error of 1.2%. Approximately half the points fall within 1% of the reference data (with 99% of the points falling within 5%) (Fig. 8). Closer to the phase boundary (along the steep portion of the curves on Fig. 8), errors can be much higher depending on whether a gaseous phase or liquid phase volume is computed, because (as discussed earlier) the vapor pressure curve of CO_2 is not accurately reproduced. In this case, the saturation pressure is reproduced within ~2 bars from the reference data of Span and Wagner (1996) (or Angus et al., 1976). Using a_{CO2} and b_{CO2} determined in this way (Table 1) and Eqn. B7 (Appendix B), fugacity coefficients for pure CO_2 could be reproduced with a mean absolute deviation of 0.6% from published reference data (Angus et al., 1976)[3] and no deviations > 2% (Fig. 9).

Once values of a_{CO2} and b_{CO2} were obtained, the molecular interaction parameters $a_{H2O\text{-}CO2}$ and b_{H2O}, as well as $K^0_{CO2(g)}$, $K^0_{CO2(l)}$, and $\bar{V}_{CO2}$, were determined by inverting simultaneously the mutual solubility data given in Appendix A. Initial guess values for K^0_{CO2} (gas and liquid) and $\bar{V}_{CO2}$ were computed using SUPCRT92 (Johnson et al., 1992) (Table 2), and initial guess values for interaction parameters were taken from King et al. (1992). A series of successive calibrations were performed, each time decreasing the number of fixed parameters. The values of $a_{H2O\text{-}CO2}$ and b_{H2O} obtained in this way

[2] The authors plan to submit their routine for publication. Until then, it is available directly from the lead author.

[3] Span and Wagner (1996) do not tabulate fugacity coefficients; within the *P-T* range considered here, their CO_2 densities and those reported by Angus et al. (1976) typically agree within < 0.1%.

Table 2. Equilibrium constants (K^0) and average partial molar volumes as defined through Eqn. 1 to 3, and regression parameters for $\log(K^0)_{T,\ 1\ bar} = a + bT + cT^2 + dT^3$ with temperature in °C. Uncertainty is shown for fitted data only, and represents the 95% confidence interval from the model calibration.

	$\log(K^0)_{T,1bar}$								
Species	15	25	31	40	50	75	100	$\bar{V}_i$(cm^3/mol)	Reference
H_2O	–1.768	–1.499	–1.348	–1.133	–0.910	–0.417	–0.006	18.1[a]	Harvey et al. (2003)
$CO_{2(g)}$	1.372	1.481	1.541	1.623	1.705	1.861	1.948	32.6	This study (see text)
	(±0.01)	(±0.01)	(±0.01)	(±0.01)	(±0.02)	(±0.02)	(±0.03)	(±1.3)	
	—	—	—	—	1.703	1.860	1.951	28.6–35.1	Carroll and Mather (1992)[b]
	—	—	—	—	—	—	1.954	—	Müller et al. (1988)[b]
	1.347	1.472	1.539	1.628	1.713	1.875	1.981	—	Crovetto (1991)[b]
	1.339	1.469	1.537	1.627	1.712	1.871	1.969	33.8[d]	SUPCRT92 (see text)
$CO_{2(l)}$	1.362[c]	1.477[c]	1.541[c]	—	—	—	—	32.6	This study (see text)
	(±0.02)	(±0.02)	(±0.03)						
$CO_{2(l)/(g)}$	1.347[c]	1.474[c]	—	1.628	—	—	—	32.0	King et al. (1992)[b]

	Regression coefficients			
Species	*a*	*b*	*c*	*d*
H_2O (fitted *T* range: 10–110°C)	–2.209	3.097×10^{-2}	-1.098×10^{-4}	2.048×10^{-7}
$CO_{2\ (g)}$ (fitted *T* range: 12–110°C)	1.189	1.304×10^{-2}	-5.446×10^{-5}	0.0
$CO_{2\ (l)}$ (fitted *T* range: 12–31°C)	1.169	1.368×10^{-2}	-5.380×10^{-5}	0.0

[a] Average of values (between 17.5 and 18.9) in the range $T = 280$ to 380 K and $P = 1$ to 601 bar at 10-K and 10-bar increments.
[b] Converted from Henry's law constants K_H using Eq. 9 for activities, yielding $\log(K) = \log(55.508 \times K_H)$.
[c] At these temperatures, the fitted solubility data reflect a liquid CO_2-rich phase.
[d] Average of values computed with SUPCRT92 between 15 and 100°C and from 1 to 500 bar.

(Table 1) are slightly higher than those reported by King et al. (1992) (who report $a_{H2O\text{-}CO2} = 7.67 \times 10^7$ bar cm^6 K$^{0.5}$ mol^{-2} and $b_{H2O} = 16.6$ cm^3/mol). These values reflect the assumption of infinite dilution of H_2O in the compressed gas phase and should be used only with the present solubility model. The estimated values of $K^0_{CO2(g)}$, $K^0_{CO2(l)}$, and $\bar{V}_{CO2}$ are within the range of values from other studies (Table 2) and further discussed below.

Using the parameters calibrated in this way (Tables 1 and 2), fitted experimental H_2O solubilities were reproduced with a mean absolute error of ~5% and individual errors < 5% for 73% of the data points. The fitted experimental CO_2 solubilities were reproduced with a mean absolute error of ~1.8% and with half the data points within 1%.

5. DISCUSSION AND CONCLUSIONS

Calculated mutual solubilities using Eqn. 11 to 14, B1, B2 and B7, and parameters presented in Tables 1 and 2, are shown as solid lines on Figures 4 to 7. Ideal solubilities of H_2O in the compressed gas phase (calculated as $y_{H2O} = P^0_{saturation\ H2O}/P_{total}$) are also shown on these figures and clearly indicate that the assumption of ideal mixing for water in the CO_2-rich phase leads to large discrepancies.

We mentioned above that the trend of CO_2 solubility with pressure at given subcritical temperatures reflects two distinct solubility curves, one for liquid CO_2 and the other for gaseous CO_2. These two solubility curves should cross exactly at the phase transition point. However, because the Redlich-Kwong equation cannot precisely predict the location of the phase change in *P*-*T* space, the model does not switch from the gas to the liquid solubility curve exactly where it should (in this case, the liquid solubility curve extends slightly into metastable space). This does not affect the shape of each individual solubility curve (gas or liquid), nor does it affect the fit of the experimental data. It only results in a small jump in the computed CO_2 solubility at the phase transition point (<0.1 mol.%), noticeable only on subcritical isotherms computed using small pressure increments (less than a couple bars or so) across the phase boundary.

From 12 up to 50°C, agreement between calculated and experimental solubilities is quite good and generally within a few percent up to pressures near 600 bar (Figs. 4 and 5). At 75 and 100°C and pressures above 50 bar, the available H_2O solubility data become scattered (Figs. 6 and 7), and the accuracy of the model is more difficult to evaluate. The 93°C data of Gillepsie and Wilson (1982) are reproduced within 7% up to 100 bar. At 200 bar, however, the calculated H_2O solubility is higher by ~17% than the value reported by these authors (Fig. 7). The 100°C data in Figure 7 include points from Greenwood and Barnes (1966) that were not included in the data inversion (nor in Appendix A) because they appear to have been extrapolated from the work of Wiebe and Gaddy (1941). The only other H_2O solubility data at 100°C and pressure above 100 bar are those reported by Tödheide and Frank (1963), which were reported with a low precision of ~±1 mol.%.

To further evaluate the model accuracy in this general temperature range, solubilities reported for 110°C by Takenouchi and Kennedy (1964) were also considered (Fig. 7). These data follow a more defined trend than the 100°C data. However, for H_2O solubilities, this trend clearly cannot be reproduced by the calculations. In absence of more consistent experimental data, model results at higher temperatures were also compared to

solubilities calculated using the Geofluids model (Duan et al., 1992, as implemented in their website calculator http://geotherm.ucsd.edu/geofluids/) (Fig. 7), which uses an accurate equation of state. Their model cannot reproduce H_2O solubilities of Takenouchi and Kennedy (1964) at 110°C either, and yields results similar to ours in this temperature range. Both models agree reasonably well at 110°C (Fig. 7), although the Geofluids model becomes less accurate in terms of solubilities at lower temperatures (this model mostly covers temperatures and pressures much larger than considered here). Volumes of the compressed gas phase calculated with both models at 100 to 110°C and 500 to 600 bar agree within 2%.

As the H_2O mole fraction in the compressed gas phase keeps increasing with temperature, the assumption of infinite H_2O dilution should eventually break down. Therefore, calculated H_2O solubilities would be expected to become progressively less accurate as temperature increases. This could be a reason for the poor H_2O solubility fit at 110°C. However, the similarity of our 110°C results with those of the Geofluids model suggest that this may not be the case. Also, Spycher et al. (1988) already pointed out difficulties in fitting smoothly the 110°C data of Takenouchi and Kennedy (1964) with other data from the literature. This suggests there could be problems with the 100 to 110°C data, in addition to the calculation limitations.

Because the mutual solubilities of CO_2 and H_2O were fitted simultaneously, the CO_2 log(K) values determined in this way reflect actual data for both the CO_2- and H_2O-rich phases. However, these solubility constants reflect the use of average CO_2 and H_2O partial molar volumes over the entire P-T range of interest. In addition, the fitted equilibrium constants reflect the assumptions made regarding the activities of water and $CO_{2(aq)}$ and other uncertainties associated with the parameters necessary to compute fugacities. Therefore, these constants should be used only with other parameters given in Tables 1 and 2.

No claims are made that the CO_2 solubility constants fitted in this study are more accurate than other values shown in Table 2. Our log(K) value at 100°C matches closely the values derived from Henry's law constants reported by both Müller et al. (1988) and Carroll and Mather (1992). However, each data source has its own share of assumptions and potential problems. Crovetto (1991) used a more comprehensive set of aqueous solubility data, but had to calculate water mole fractions in the gas phase (rather than rely on measured data) to compute her values of Henry's law constants. This author also omitted data in our P-T range of interest (specifically, points above 2 bar and between 0 and 80°C) because of difficulties in evaluating data near the CO_2 critical point. Carroll and Mather (1992) used measured gas-phase compositions to derive Henry's law constants, but did not cover data below 50°C. Log(K) values derived from their reported Henry's law constants between 50 and 100°C are in close agreement with our estimated log(K) values (Table 2). However, these authors fitted each isotherm separately, and obtained inconsistent trends of partial molal volume variation with temperature, and a value possibly too low at 100°C (28.6 cm^3/mol) (e.g., Garcia, 2001). These authors also had to exclude the data of Müller et al. (1988) in their analyses to obtain meaningful volume values at 100°C. This may be partly caused by the fact that for each isotherm, these authors attempted to fit an activity model for $CO_{2(aq)}$ (a Margules parameter) in addition to the partial molal volume and the Henry's law constant. This could have resulted in "overfitting" the data because the activity of $CO_{2(aq)}$ is likely to remain very close to unity at the small concentrations considered. Also note that the log(K) values derived from the Henry's law constants reported by King et al. (1992) and Crovetto (1991) at 15°C are identical. However, the study of King et al. (1992) involved liquid CO_2 below the critical temperature, whereas Crovetto (1991) considered only experimental studies in which gaseous CO_2 was present. Therefore, it is fortuitous that some of the log(K) values in Table 2 match exactly. The general agreement between the various solubility constant values would seem to indicate that aqueous solubility differences caused by the CO_2 phase change in the 12 to 31°C temperature range are within the range of errors introduced by the various correlation approaches and experimental procedures.

The method presented here to compute the mutual solubilities of H_2O and CO_2 is essentially a reformulation of the standard approach of equating fugacities to calculate P-T-X properties of phases at equilibrium. The formulation relies on true equilibrium constants and could be easily extended to moderately saline solutions through the use of published activity models for water and aqueous species. Simplifications resulting from the assumption of infinite dilution of H_2O in the CO_2-rich phase significantly improves computing efficiency, because an iterative solution scheme is not required. This assumption was originally shown by King et al. (1992) to work well at temperatures up to 40°C for the CO_2-H_2O system. Our study suggests that this approximation can be made to temperatures of at least 100°C. The equation of state adopted for this study is adequate to reproduce mutual solubilities typically within a few percent of experimental data. Compressibility factors a couple bars away from the CO_2 vapor pressure curve are reproduced mostly within 5% of reference data. This equation of state is not intended to calculate an accurate vapor-pressure curve, or to derive accurate thermodynamic properties. The approach implemented here was intended for efficient calculation of mutual solubilities in numerical models used to study the feasibility of CO_2 geologic sequestration. It is also useful for other practical applications involving geochemical systems at temperatures between 12 and 100°C and pressures up to 600 bar.

Acknowledgments—The authors wish to acknowledge John Apps, George Moridis, Sonia Salah, and Julio Garcia for constructive discussions and comments during the course of this study, and Dan Hawkes for editorial support. The authors also thank I-Ming Chou, Jean Dubessy, James Blencoe and Simon Marshall for their journal peer-reviews and useful comments. We also wish to acknowledge our Associate Editor, David Wesolowski, for his handling of the manuscript and additional suggestions. This work was supported by the US Department of Energy through the Office of Basic Energy Sciences under Contract No. DE-AC03-76SF00098. One author (JEK) wishes to acknowledge support from the Australian Petroleum Cooperative Research Center's GEODISC project.

Associate editor: D. J. Wesolowski

REFERENCES

Adamson A. W. (1979) *A Textbook of Physical Chemistry*. 2nd. ed. Academic Press, New York.

Anderson G. K. (2002) Solubility of carbon dioxide in water under incipient clathrate formation conditions. *J. Chem. Eng. Data* **47**, 219–222.

Angus S., Armstrong B., and De Reuck K. M. (1976) *International Thermodynamic Tables of the Fluid State. 3. Carbon Dioxide.* Int. Union of Pure and Applied Chemistry. Pergamon Press, New York.

Bamberger, A., Sieder, G., Maurer, G., 2000. High-pressure (vapor+liquid) equilibrium in binary mixtures of (carbon dioxide + water or acetic acid) at temperatures from 313 to 353 K. J. Supercritical Fluids, **17,** 97–100.

Briones J. A., Mullins J. C., and Thies M. C. (1987) Ternary phase equilibria for acetic acid-water mixtures with supercritical carbon dioxide. *Fluid Phase Equilib.* **36**, 235–246.

Carroll J. J. and Mather A. E. (1992) The system carbon dioxide-water and the Krichevsky-Kasarnovsky equation. *J. Solut. Chem.* **21**, 607–621.

Coan C. R. and King A. D. Jr. (1971) Solubility of water in compressed carbon dioxide, nitrous oxide, and ethane. Evidence for hydration of carbon dioxide and nitrous oxide in the gas phase. *J. Am. Chem. Soc.* **93**, 1857–1862.

Crovetto R. (1991) Evaluation of solubility data for the system CO_2-H_2O from 273 K to the critical point of water. *J. Phys. Chem. Ref. Data* **20**, 575–589.

Denbigh K. (1983) *The Principles of Chemical Equilibrium*. 4th. ed. Cambridge University Press, Cambridge, UK.

deSantis R., Breedveld G. J. F., and Prausnitz J. M. (1974) Thermodynamic properties of aqueous gas mixtures at advanced pressures. *Ind. Chem. Proc. Des. Dev.* **13,** *4*, 374–377.

Dohrn R., Bünz A. P., Devlieghere F., and Thelen D. (1993) Experimental measurements of phase equilibria for ternary and quaternary systems of glucose, water, CO_2 and ethanol with a novel apparatus. *Fluid Phase Equilib.* **83**, 149–158.

Doherty J. (2002) *PEST—Model-Independent Parameter Estimation*. Watermark Numerical Computing, Brisbane, Australia.

D'Souza R., Patrick J. R., and Teja A. S. (1988) High pressure phase equilibria in the carbon dioxide-n-hexadecane and carbon dioxide-water systems. *Can. J. Chem. Eng.* **66**, 319–323.

Duan Z., Møller N., and Weare J. H. (1992) An equation of state for the CH_4-CO_2-H_2O system: II. Mixtures from 50 to 1000°C and 0 to 1000 bars. *Geochim. Cosmochim. Acta* **56**, 2619–2631.

Evelein K. A., Moore R. G., and Heidemann R. A. (1976) Correlation of the phase behavior in the systems hydrogen sulfide-water and carbon dioxide-water. *Ind. Eng. Chem. Proc. Des. Dev.* **15,** *3,* 423–428.

Fan S.-S. and Guo T.-M. (1999) Hydrate formation of CO_2-rich binary and quaternary gas mixtures in aqueous sodium chloride solutions. *J. Chem. Eng. Data* **44,** *4*, 829–832.

Garcia J. E (2001) *Density of Aqueous Solutions of CO_2.* LBNL Report 49023, Lawrence Berkeley National Laboratory, Berkeley, CA.

Gillepsie P. C., and Wilson G. M. (1982) *Vapor-Liquid and Liquid-Liquid Equilibria: Water-Methane, Water-Carbon Dioxide, Water-Hydrogen Sulfide, Water-nPentane, Water-Methane-nPentane*. Research report RR-48, Gas Processors Association, Tulsa, OK.

Greenwood H. J, Barnes H. L (1966) Binary mixtures of volatile components. In *Handbook of Physical Constants* (ed. S. P. Clark). The Geological Society of America Memoir 97.

Hala E., Pick J., Fried V., and Vilim O. (1967) Vapor-Liquid Equilibrium. Pergamon Press, New York.

Harvey A. H., Perkin A. P., and Klein S. A. (2000) NIST Standard Reference Database 10, Version 2.2. International Association for the Properties of Water and Steam (IAPWS) 95. U.S. Dept. of Commerce, National Institute of Standards and Technology, Standard Reference Data Program, Gaithersburg, MD.

Helgeson H. C. and Kirkham D. H. (1974) Theoretical prediction of the thermodynamic behavior of aqueous electrolytes at high pressures and temperatures: I. Summary of the thermodynamic/electrostatic properties of the solvent. *Am. J. Sci.* **274**, 1089–1198.

Helgeson H. C., Kirkham D. H., and Flowers G. C. (1981) Theoretical prediction of the thermodynamic behavior of aqueous electrolytes at high pressures and temperatures: IV. Calculation of activity coefficients, osmotic coefficients, and apparent molal and standard and relative partial molal properties to 600°C and 5 kb. *Am. J. Sci.* **281**, 1249–1516.

Jackson K., Bowman L. E., and Fulton J. L. (1995) Water solubility measurements in supercritical fluids and high-pressure liquids using near-infrared spectroscopy. *Anal. Chem.* **67**, 2368–2372.

Johnson J. W., Oelkers E., and Helgeson H. C. (1992) SUPCRT92: A software package for calculating the standard molal thermodynamic properties of minerals, gases, aqueous species and reactions from 1 to 5000 bar and 0 to 1000°C. *Comput. Geosci.* **18**, 899–947.

Kerrick D. M. and Jacobs G. K. (1981) A modified Redlich-Kwong equation for H_2O, CO_2 and H_2O-CO_2 mixtures at elevated pressures and temperatures. *Am. J. Sci.* **281**, 735–767.

King M. B., Mubarak A., Kim J. D., and Bott T. R. (1992) The mutual solubilities of water with supercritical and liquid carbon dioxide. *J. Supercrit. Fluids* **5**, 296–302.

Lemmon E. W., McLinden M. O., and Friend D. G. (2003) Thermophysical properties of fluid systems. In *NIST Chemistry WebBook*, NIST Standard Reference Database Number 69 (eds. P. J. Linstrom and W. G. Mallard). National Institute of Standards and Technology, Gaithersburg MD.

Mäder U. K. (1991) H_2O-CO_2 mixtures: A review of P-V-T-X data and an assessment from a phase equilibrium point of view. *Can. Mineral.* **29**, 767–790.

Müller G., Bender E., and Maurer G. (1988) Das Dampf-Flüssigkeits-gleichgewicht des Ternären Systems Ammoniak-Kohlendioxid-Wasser bei Hohen Wassergehalten im Bereich Zwischen 373 und 473 Kelvin. *Berichte der Bunsen-Gesellshaft für Physikalische Chemie* **92**, 148–160.

Ng H.-J. and Robinson D. B. (1985) Hydrate formation in systems containing methane, ethane, propane, carbon dioxide or hydrogren sulfide in the presence of methanol. *Fluid Phase Equilib.* **21**, 145–155.

Nickalls R. W. D. (1993) A new approach to solving the cubic: Cardan's solution revealed. *Math. Gazette* **77**, 354–359.

Peng D.-Y. and Robinson D. B. (1976) A new two-constant equation of state. *Ind. Eng. Chem. Fundament.* **15**, 59–64.

Prausnitz J. M., Lichtenthaller R. N., and De Azedevo E. G. (1986) Molecular Thermodynamics of Fluid Phase Equilibria. Prentice Hall, New York.

Pruess K. and Garcia J. (2002) Multiphase flow dynamics during CO_2 disposal into saline aquifers. *Environ. Geol.* **42**, 282–295.

Redlich O. and Kwong J. N. S. (1949) On the thermodynamics of solutions. V. An equation of state. Fugacities of gaseous solutions. *Chem. Rev.* **44**, 233–244.

Rosenbauer R. J., Bischoff J. L., and Koksalan T. (2001) An experimental approach to CO_2 sequestration in saline aquifers: Application to Paradox Valley, CO. *Eos: Trans. Am. Geophys. Union* **82,** *47,* Fall Meet. Suppl., Abstract V32B-0974, 2001.

Sako T., Sugeta T., Nakazawa N., Obuko T., Sato M., Taguchi T., and Hiaki T. (1991) Phase equilibrium study of extraction and concentration of furfural produced in reactor using supercritical carbon dioxide. *J. Chem. Eng Jpn.* **24**, 449–454.

Shyu G.-S., Hanif N. S. M., Hall K. R., and Eubank P. T. (1997) Carbon dioxide-water phase equilibria results from the Wong-Sandler combining rules. *Fluid Phase Equilib.* **130**, 73–85.

Song K. Y. and Kobayashi R. (1987) Water content of CO_2 in equilibrium with liquid water and/or hydrates. *SPE Form. Eval.* **2**, 500–508.

Span R. and Wagner W. (1996) A new equation of state for carbon dioxide covering the fluid region from the triple-point temperature to 1100K at pressures up to 800 MPa. *J. Phys. Chem. Ref. Data* **25,** *6*, 1509–1596.

Spycher N. F. and Reed M. H. (1988) Fugacity coefficients of H_2, CO_2, CH_4, H_2O and H_2O-CO_2-CH_4 mixtures: A virial equation treatment for moderate pressures and temperatures applicable to hydrothermal boiling. *Geochim. Cosmochim. Acta* **52**, 739–749.

Takenouchi S. and Kennedy G. C. (1964) The binary system H_2O-CO_2 at high temperatures and pressures. *Am. J. Sci.* **262**, 1055–1074.

Teng H., Yamasaki A., Chun M.-K., and Lee H. (1997) Solubility of liquid CO_2 in water at temperatures from 278 K to 293 K and pressures from 6.44 MPa to 29.49 MPa and densities of the corresponding aqueous solutions. *J. Chem. Thermodyn.* **29**, 1301–1310.

Tödheide K. and Frank E. U. (1963) Das Zweiphasengebiet und die Kritische Kurve im System Kohlendioxid-Wasser bis zu Drucken von 3500 bar. *Z. Phys. Chemie, Neue Folge.* **37**, 387–401.

U.S. Department of Energy(1999) *Carbon Sequestration Research and Development*. Report DOE/SC/FE-1, U.S. Department of Energy, Office of Science, Office of Fossil Energy, Washington, DC.

Wagner W. and Pruβ A. (2002) The IAPW formulation 1995 for the thermodynamic properties of ordinary water substance for general scientific use. *J. Phys. Ref. Data* **31**, 387–535.

Wendland M., Hasse H., and Maurer G. (1999) Experimental pressure-temperature data on three- and four-phase equilibria of fluid, hydrate, and ice phases in the system carbon dioxide-water. *J. Chem. Eng. Data* **44,** *5*, 901–906.

Wiebe R. and Gaddy V. L. (1939) The solubility in water of carbon dioxide at 50, 75, and 100°, at pressures to 700 atmospheres. *J. Am. Chem. Soc.* **61**, 315–318.

Wiebe R. and Gaddy V. L. (1940) The solubility of carbon dioxide in water at various temperatures from 12 to 40° and at pressures to 500 atmospheres: Critical phenomena. *J. Am. Chem. Soc.* **62**, 815–817.

Wiebe R. and Gaddy V. L. (1941) Vapor phase composition of carbon dioxide-water mixtures at various temperatures and at pressures to 700 atmospheres. *J. Am. Chem. Soc.* **63**, 475–477.

Appendix A

A.1. Mutual Solubilities of CO_2 and H_2O: Experimental Data from 12 to 110°C and from 1 to 700 bar

T (°C)	*P* (bar)	y_{H2O} (‰)	x_{CO2} (%)	Ref. gas	Ref. liq.
12	34.5	0.6030		18	
12	50.7		2.777		3
12	76.0		2.837		3
12	101.3		2.871		3
12	152.0		2.993		3
12	202.7		3.098		3
12	304.0		3.196		3
13.17	137.9	3.3627		18	
13.78	82.8	2.7852		18	
15	51.7	2.22		1	
15	60.8		2.658		1
15	64.4		2.69		11
15	70.9		2.716		1
15	76.0	2.35	2.729	1	1
15	98.7		2.80		11
15	101.3	2.41	2.757	1	1
15	121.6		2.828		1
15	126.7	2.55		1	
15	131.7		2.840		1
15	147.7		2.96		11
15	152.0	2.62	2.886	1	1
15	157.1		2.902		1
15	177.3	2.72	2.960	1	1
15	196.8		3.09		11
15	202.7	2.80	3.013	1	1
15	243.2		3.070		1
15	245.8		3.19		11
15	294.9		3.27		11
15.56	20.7	1.0656		18	
15.56	52.4	0.6400 (g)		18	
15.56	52.4	1.1200 (l)		18	
15.6	50.7	0.819	2.58	13	13
15.6	101.4	2.78	2.42	13	13
15.6	202.7	2.92	2.61	13	13
17	48.3	0.8229		18	
18	25.3		1.544		3
18	50.7		2.510		3
18	76.0		2.649		3
18	101.3		2.659		3
18	152.0		2.793		3
18	202.7		2.901		3
18	304.0		3.063		3
20	34.5	1.0010		18	
20	58.8	2.61		1	
20	64.4		2.50		11
20	65.9		2.531		1
20	70.9	2.72		1	
20	76.0	2.76	2.563	1	1
20	81.1	2.78		1	
20	96.3		2.597		1
20	98.7		2.58		11
20	101.3	2.93	2.625	1	1
20	126.7	2.87		1	
20	136.8		2.689		1
20	141.9	3.07		1	
20	146.9		2.727		1
20	147.7		2.75		11
20	152.0	3.20	2.743	1	1
20	177.3	3.22	2.807	1	1
20	196.8		2.93		11
20	202.7	3.34	2.847	1	1
20	217.9		2.945		1
20	245.8		3.04		11
20	294.9		3.12		11
20.2	57.9	0.8999 (g)		18	
20.2	57.9	1.5000 (l)		18	
21	100		2.59		10
21	300		2.94		10
21	600		3.36		10
21.1	6.9	4.3276		18	
25	1.0	28.6		2	
25	22.7	1.95		5	
25	25.3	1.64		2	
25	29.8	1.63		5	
25	30.0	1.67		5	
25	37.3	1.45		5	
25	37.4	1.49		5	
25	48.3	1.2787		18	
25	50.7	1.28	2.10	13	13
25	50.7	1.29	2.142	2	3
25	65.9	3.00		1	
25	70.9	3.07		1	
25	76.0		2.444		3
25	76.0	3.09	2.445	1	1
25	82.8	3.0152		18	
25	91.2	3.14		1	
25	101.3	3.27	2.510	1	1
25	101.3	3.32	2.488	2	3
25	101.4	3.36	2.49	13	13
25	103.4	3.3739		18	
25	111.5	3.37		1	
25	126.7	3.41		1	
25	136.8		2.582		1
25	141.9	3.44		1	
25	152.0	3.54	2.603	1	1
25	152.0	3.60		2	
25	177.3	3.69	2.672	1	1
25	202.7	3.76	2.57	13	13
25	202.7	3.78	2.734	1	1
25	202.7	3.77		2	
25	405.3		3.011		3
25	456.0	4.01		2	
25	481.3	3.99		2	
25	506.6	3.97		2	
26.67	66.9	1.2700 (g)		18	
26.67	66.9	1.9541 (l)		18	
29.4	55.2	1.57	2.03	13	13
29.4	101.4	3.89	2.39	13	13
29.4	202.7	4.36	2.63	13	13
29.5	71.7	1.4981 (g)		18	
29.5	71.7	2.1940 (l)		18	

T (°C)	P (bar)	y_{H2O} (‰)	x_{CO2} (%)	Ref. gas	Ref. liq.
31.04	1.0	39.8		2	
31.04	25.3	2.28	1.127	2	3
31.04	50.7	1.61	1.904	2	3
31.04	76.0		2.303		3
31.04	101.3	3.65	2.368	2	3
31.04	152.0		2.476		3
31.04	202.7	4.21	2.567	2	3
31.04	405.3	4.77	2.871	2	3
31.04	506.6	4.80	3.014	2	3
31.04	532.0	4.75		2	
31.04	557.3	4.78		2	
31.05	6.9	6.94	0.331	13	13
31.05	25.3	2.39	1.056	13	13
31.05	50.7	1.63	1.817	13	13
31.05	101.4	4.08	2.41	13	13
31.05	202.7	4.50	2.62	13	13
31.06	73.9	2.1079		18	
35	25.3		1.030		3
35	50.7		1.754		3
35	76.0		2.189		3
35	91.2	3.84		1	
35	101.3	4.07	2.288	1	3
35	111.5	4.14		1	
35	126.7	4.35		1	
35	136.8	4.40		1	
35	152.0	4.57	2.394	1	3
35	202.7	4.98	2.495	1	3
35	405.3		2.792		3
35	506.6		2.963		3
40	25.3		0.9253		3
40	50.7		1.609		3
40	76.0		2.032		3
40	101.3	4.28	2.186	1	3
40	111.5	4.40		1	
40	126.7	4.67	2.256	1	3
40	152.0	5.07	2.308	1	3
40	177.3	5.43		1	
40	202.7	5.80	2.488	1	3
40	405.3		2.726		3
40	506.6		2.868		3
50	1.0	116		2	
50	17.3	8.41		5	
50	25.3	6.20	0.774	2	4
50	25.5	5.95		5	
50	25.8	5.98		5	
50	36.4	4.66		5	
50	36.4	4.63		5	
50	40.5	4.6	1.09	19	19
50	46.3	3.96		5	
50	50.6	3.6	1.37	19	19
50	50.7	3.83	1.367	2	4
50	60.6	3.7	1.61	19	19
50	60.8	3.57		2	
50	68.2	3.39	1.651	14	14
50	70.8	3.4	1.76	19	19
50	75.3	3.45	1.750	14	14
50	76.0	3.50	1.779	2	4
50	80.8	3.4	1.90	19	19
50	87.2	3.64	1.768	14	14
50	90.9	4.1	2.00	19	19
50	100.6	4.29		14	
50	100.9	4.5	2.05	19	19
50	101	5.47	2.075	17	17
50	101.3	4.36	2.081	14	14
50	101.3	4.49	2.018	2	4
50	101.33	5.5	1.98	15	15
50	111.0	5.0	2.10	19	19
50	121.0	5.5	2.14	19	19
50	122.1	5.43	2.096	14	14
50	126.7		2.106		4
50	141.1	6.1	2.17	19	19
50	147.5	6.08	2.215	14	14
50	147.5		2.207		14
50	152.0	6.10	2.174	2	4
50	152.0	7.9	2.10	15	15
50	176.8	6.43	2.262	14	14
50	200	10	2.3	6	6
50	201	6.82	2.347	17	17
50	202.7	6.77	2.289	2	4
50	301	7.82	2.514	17	17
50	304.0		2.457		4
50	344.8	7.5		8	
50	405.3	7.59	2.606	2	4
50	500	10	2.8	6	6
50	608.0	7.93	2.868	2	4
50	709.3	8.01	2.989	2	4
60	40.5	6.6	0.96	19	19
60	50.6	5.5	1.21	19	19
60	60.6	5.5	1.38	19	19
60	70.8	5.1	1.57	19	19
60	80.8	5.0	1.66	19	19
60	90.9	4.7	1.79	19	19
60	100.9	4.9	1.86	19	19
60	111.0	5.3	1.95	19	19
60	121.0	5.8	2.01	19	19
60	141.1	7.8	2.08	19	19
75	1.0	301		2	
75	6.9	60.14	0.149	13	13
75	25.3	18.16	0.542	13	13
75	25.3	10.6	0.545	2	4
75	23.3	20.0		5	
75	37.4	12.5		5	
75	37.5	12.6		5	
75	50.7	10.87	1.006	13	13
75	50.7		1.002		4
75	51.3	10.4		5	
75	51.5	10.2		5	
75	76.0		1.351		4
75	101.3	8.29	1.630	2	4
75	101.33	7.4	1.56	15	15
75	101.4	7.27	1.616	13	13
75	103.4	6.3	1.91	16	16
75	111.5	8.11		2	
75	126.7	8.55		2	
75	152.0	9.56	1.937	2	4
75	152.0	9.0	1.88	15	15
75	153.1	7.5	1.92	16	16
75	202.7	9.38	2.09	13	13
75	202.7	11.3	2.098	2	4
75	209.4	8.4		16	
75	304.0		2.317		4
75	344.8	13.3		8	
75	405.3	13.19	2.498	2	4
75	608.0	13.93		2	
75	709.3	14.00	2.933	2	4
80	40.5	14.3	0.80	19	19
80	60.6	10.9	1.14	19	19
80	70.8	10.4	1.28	19	19
80	80.8	9.7	1.40	19	19
80	90.9	9.2	1.51	19	19
80	100.9	9.3	1.60	19	19
80	111.0	9.0	1.72	19	19
80	121.0	9.6	1.76	19	19
80	131.0	10.0	1.84	19	19
93.3	6.9	120.3	0.0973	13	13
93.3	25.3	34.71	0.435	13	13

T (°C)	P (bar)	y_{H2O} (‰)	x_{CO2} (%)	Ref. gas	Ref. liq.
93.3	50.7	19.70	0.846	13	13
93.3	101.4	13.74	1.45	13	13
93.3	202.7	14.32	2.06	13	13
100	3.25	288	0.045	12	12
100	6.00	155	0.098	12	12
100	9.20	107	0.159	12	12
100	11.91	77.0	0.208	12	12
100	14.52	69.0	0.261	12	12
100	18.16	54.0	0.328	12	12
100	23.07	45.0	0.414	12	12
100	25.3		0.4294		4
100	36.8	32.8		5	
100	37.2	32.3		5	
100	44.8	27.7		5	
100	44.8	27.4		5	
100	50.7		0.812		4
100	51.5	24.8		5	
100	51.5	25.1		5	
100	76.0		1.135		4
100	101.3		1.400		4
100	152.0		1.794		4
100	200.0	29	2.0	6	6
100	202.7		2.023		4
100	304.0		2.318		4
100	405.3		2.537		4
100	500.0	30	2.8	6	6
100	709.3		3.002		4
110	100	44	1.40	7	7
110	200	42	2.10	7	7
110	300	52	2.40	7	7
110	400	68	2.60	7	7
110	500	86	2.80	7	7
110	600	107	3.00	7	7
110	700	128	3.15	7	7

(g) and (l) refer to H_2O solubilities reported in coexisting gaseous and liquid CO_2, respectively. References (in same order as in Figures 4-7): (1) King et al. (1992), (2) Wiebe and Gaddy (1941), (3) Wiebe and Gaddy (1940), (4) Wiebe and Gaddy (1939), (5) Coan and King (1971), (6) Tödheide and Frank (1963), (7) Takenouchi and Kennedy (1964), (8) Jackson et al. (1995), (9) not used in this Table, (10) Rosenbauer et al. (2001), (11) Teng et al. (1997), (12) Müller et al. (1988), (13) Gillepsie and Wilson (1982), (14) Briones et al. (1987), (15) D'Souza et al. (1988), (16) Sako et al. (1991), (17) Dohrn et al. (1993), (18) Song and Kobayashi (1987), (19) Bamberger et al. (2000).

APPENDIX B

B.1. Equation of State and Mixing Rules

The Redlich-Kwong equation takes the form (Redlich and Kwong, 1949)

$$P = \left(\frac{RT}{V-b}\right) - \left(\frac{a}{T^{0.5}V(V+b)}\right) \tag{B1}$$

where parameter a and b represent measures of intermolecular attraction and repulsion, respectively. V is the volume of the compressed gas phase at pressure P and temperature T, and R the is gas constant. In the standard equation, parameters a and b are derived from critical constraints. Here, we use a modified form by setting

$$a = k_0 + k_1 T \tag{B2}$$

and fitting k_0, k_1, and b to reference P-V-T data.

For mixtures, parameters a and b can be calculated by the following standard mixing rules (e.g., Prausnitz et al., 1986):

$$a_{mix} = \sum_{i=1}^{n}\sum_{j=1}^{n} y_i y_j a_{ij} \tag{B3}$$

$$b_{mix} = \sum_{i=1}^{n} y_i b_i \tag{B4}$$

where a_{mix} and b_{mix} replace a and b in Eqn. B1. For the binary H_2O-CO_2 mixture, therefore,

$$a_{mix} = y_{H2O}{}^2\, a_{H2O} + 2y_{H2O}\, y_{CO2}\, a_{H2O\text{-}CO2} + y_{CO2}{}^2\, a_{CO2} \tag{B5}$$

$$b_{mix} = y_{H2O}\, b_{H2O} + y_{CO2}\, b_{CO2} \tag{B6}$$

From these mixing rules and Eqn. B1 the fugacity coefficient, Φ_k, of component k in mixtures with other components i can be calculated as (e.g., Prausnitz et al., 1986)

$$\ln(\phi_k) = \ln\left(\frac{V}{V-b_{mix}}\right) + \left(\frac{b_k}{V-b_{mix}}\right) - \left(\frac{2\sum_{i=1}^{n} y_i a_{ik}}{RT^{1.5} b_{mix}}\right) \ln\left(\frac{V+b_{mix}}{V}\right) + \left(\frac{a_{mix} b_k}{RT^{1.5} b_{mix}^2}\right)\left[\ln\left(\frac{V+b}{V}\right) - \left(\frac{b_{mix}}{V+b_{mix}}\right)\right] - \ln\left(\frac{PV}{RT}\right) \tag{B7}$$

It is apparent from this equation that the fugacity coefficient of each component in the gas mixture depends on the mixture composition (in addition to pressure and temperature). Therefore, Eqn. B7 (and Eqn. B1 to calculate P, V, or T from two of these three variables) need to be solved simultaneously with Eqn. 11 to 14 to compute the mutual solubilities of CO_2 and H_2O. This requires an iterative scheme that can add significant burden for implementation into already computationally intensive fluid flow/transport models. However, if the assumption is made that $y_{H2O} = 0$ and $y_{CO2} = 1$ in the mixing rules in Eqn. B3 to B7 (i.e., assumption of infinite H_2O dilution in the CO_2-rich phase), the fugacity coefficients Φ_{H2O} and Φ_{CO2} can be computed in a direct, noniterative, manner. This is because a_{mix} and b_{mix} in Eqn. B5 and B6 simplify to a_{CO2} and b_{CO2}, respectively. The strongly nonideal mixing behavior is still captured through the molecular interaction parameters a_{ik} and b_k (i.e., $a_{H2O\text{-}CO2}$ and b_{H2O}) in Eqn. B7, which are used to calculate the H_2O fugacity coefficient. The parameter a_{H2O} is not needed (e.g., King et al., 1992).

B.2. Numerical Implementation

The volume of the compressed gas phase is computed by recasting Eqn. B1 as a general cubic equation in terms of volume,

$$V^3 - V^2\left(\frac{RT}{P}\right) - V\left(\frac{RTb}{P} - \frac{a}{PT^{0.5}} + b^2\right) - \left(\frac{ab}{PT^{0.5}}\right) = 0 \tag{B8}$$

then solving this equation directly using the method of Nickalls (1993). Below the critical point, this equation yields more than one volume value as it attempts to reproduce the liquid-gas phase transition (Fig. B1). The volume value to use depends on which phase, liquid or gas, is stable at a given pressure and temperature.

The volume of the gas phase, V_{gas}, is always given by the maximum root of Eqn. B8 (Fig. B1). The minimum root always provides the volume of the liquid phase, V_{liquid}. The phase transition occurs at the point where the work w_1 done from V_{gas} to V_{liquid} along a straight path is the same as the work w_2 done along the curved path depicted by Eqn. B1 (Fig. B1) (e.g., Adamson, 1979). From the work definition ($w = \int P dV$) w_1 is easily computed as

$$w_1 = P\,(V_{gas} - V_{liquid}) \tag{B9}$$

and w_2 is given by differentiating Eqn. B1 between V_{gas} and V_{liquid} to obtain

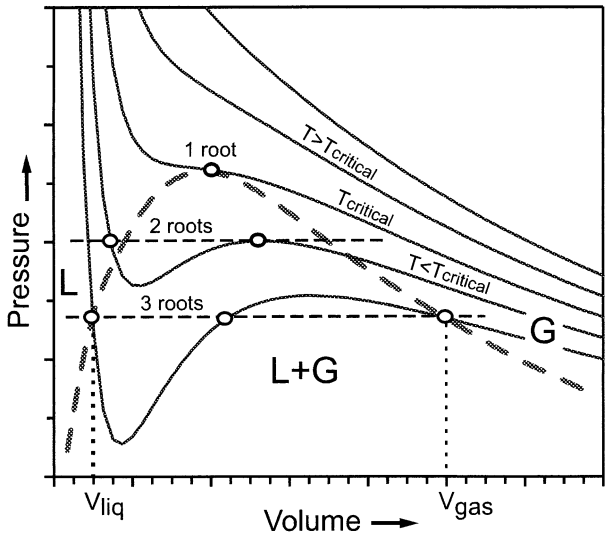

Fig. B1. Illustration of *P-V-T* relationships calculated with the Redlich-Kwong equation (Eqn. B1) or similar cubic equations of state for a pure fluid (G = gas, L = liquid, and the dashed line denotes the phase boundary). See text.

$$w_2 = RT \ln\left(\frac{V_{gas}-b}{V_{liquid}-b}\right) + \frac{a}{T^{0.5}b}\ln\left(\frac{(V_{gas}+b)V_{liquid}}{(V_{liquid}+b)V_{gas}}\right) \quad \text{(B10)}$$

For any pressure and temperature, the volume of the stable phase is then computed according to the following criteria: if $(w_2 - w_1) > 0$, then V is taken as the maximum root of Eqn. B8, and if $(w_2 - w_1) < 0$, then V is taken as the minimum root. If $(w_2 - w_1) = 0$, two phases are stable and, therefore, both roots provide a correct answer (in such case, we use the maximum root). Once the volume of the compressed gas phase is computed, it is substituted directly into Eqn. B7 to compute fugacity coefficients.